Methane production by acetate dismutation stimulated by Shewanella oneidensis and carbon materials: An alternative to classical CO2 reduction

Leilei Xiao, Fanghua Liu, Eric Lichtfouse, Peng Zhang, Dawei Feng, Fangbai Li

Chemical Engineering Journal
Volume 389, 1 June 2020, 124469
https://doi.org/10.1016/j.cej.2020.124469
Available online 15 February 2020

Methane production by acetate dismutation stimulated by *Shewanella oneidensis* and carbon materials: An alternative to classical CO_2 reduction

Leilei Xiao[a,c], Fanghua Liu[a,b,c,*], Eric Lichtfouse[d], Peng Zhang[e], Dawei Feng[a,c], Fangbai Li[f]

[a] *Key Laboratory of Coastal Biology and Biological Resources Utilization, Yantai Institute of Coastal Zone Research, Chinese Academy of Sciences, Yantai 264003, PR China*
[b] *Laboratory for Marine Biology and Biotechnology, Qingdao National Laboratory for Marine Science and Technology, Qingdao 266237, PR China*
[c] *Center for Ocean Mega-Science, Chinese Academy of Sciences, Qingdao 266071, PR China*
[d] *Aix-Marseille Univ, CNRS, IRD, INRA, Coll France, CEREGE, Avenue Louis Philibert, Aix en Provence 13100, France*
[e] *Faculty of Environmental Science & Engineering, Kunming University of Science & Technology, Kunming 650500, PR China*
[f] *Guangdong Key Laboratory of Integrated Agro-environmental Pollution Control and Management, Guangdong Institute of Eco-environmental Science & Technology, Guangzhou 510650, PR China*

HIGHLIGHTS

- Potential electric syntrophy occurred between *Shewanella oneidensis* and methanogens.
- Various technologies were used to verify methane production pathways.
- Direct acetate dismutation preference via increased exoelectrogenic activity.
- A new model for electron flow during syntrophic methanogenesis was revealed.

GRAPHICAL ABSTRACT

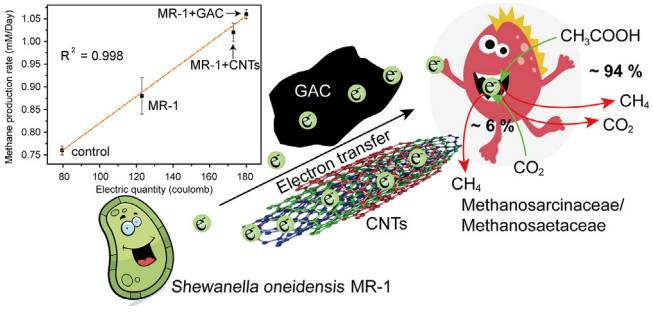

ARTICLE INFO

Keywords:
Acetoclastic methanogenesis
Independent CO_2 reduction
Shewanella oneidensis MR-1
Exogenous electron
Electron transfer
Methane production

ABSTRACT

Methane is a major greenhouse gas responsible of global warming and renewable energy, but the precise contribution of biomethane from microbial decomposition is vague because microbial mechanisms are not fully understood. CO_2 reduction and direct acetate dismutation are two main pathways for biomethane production, accounting for ~1/3 and 2/3 of produced methane in terrestrial ecosystems, respectively. A classical process explaining methane production involves CO_2 reduction by direct interspecies electron transfer (DIET). Herein, we hypothesized that methane could also be produced by direct acetate dismutation by syntrophy between electron-donating *Shewanella oneidensis* MR-1 and electron-accepting methanogens. We tested the effect of two conducting carbon materials, granular activated carbon and carbon nanotubes, on methane production. The electrical activity was monitored with a microbial fuel cell. We used CH_3F, ^{13}C labelling, thermodynamics, DNA analysis and modelling to elucidate the mechanism. Results show that the rate of methane production increased by 29.0% using *S. oneidensis* MR-1, and by 36.2–40.7% using *S. oneidensis* MR-1 and conducting materials. ^{13}C labelling shows that about 94% of methane is produced by acetate dismutation. Findings further show that acetate dismutation is enhanced by exoelectrogenic activity, thus suggesting that electrons from *S. oneidensis* MR-1 are used to convert methyl groups into methane. Overall our results disclose DIET-acetate dismutation as an alternative mechanism of biomethane production, which is highly stimulated by carbon-based conductive

* Corresponding author at: Yantai Institute of Coastal Zone Research, 17 Chunhui Road, Laishan District, Yantai, Shandong 264003, PR China.
E-mail address: fhliu@yic.ac.cn (F. Liu).

materials. These findings are of significance for further understanding methanogenic progresses with the involvement of electroactive microorganisms in natural environments and artificial anaerobic systems.

1. Introduction

As a potent greenhouse gas and feasible source of renewable energy, methane takes an active part in carbon and energy cycles. Biomethane is produced in anaerobic environments such as soils, sediments, and waste treatment plants [1–3]. Since methanogenesis is the final step of organic matter degradation, limiting methanogenesis by geoengineering would induce accumulation of high amounts of organic C in soils and sediments, and thus would favor C sequestration. On the other hand, optimizing biomethane production is needed for the development of sustainable fuels. Nonetheless, microbial mechanisms ruling biomethane generation are not fully understood. The classical pathway for biomethane production is CO_2 reduction involving H_2 as reducing agent [4]. Yet the H_2 diffusion rate is slow, which decreases the rate of methane generation. To optimize methane production, alternative strategies are thus needed. Here, recent studies have revealed an alternative mechanism, named direct interspecies electron transfer (DIET), which do not rely on the diffusion of gaseous compounds. DIET has been identified in wastewater digesters [5], and in pure cultures of *Geobacter* and methanogens [6,7].

Methanogenesis can be accelerated by fostering the syntrophy between electron-donating and electron-accepting partners. For example, methanogenesis is accelerated when either the electrical performance of *Geobacter* or the electrode potential are enhanced [8,9]. Methane production is also augmented by the addition of conductive materials, which increase the conductivity between electron-donating microbes and methanogens [10–13]. Actually, DIET coupled with CO_2 reduction (DIET-CO_2) is considered as the sole mechanism explaining methane production by electric syntrophy [14–16]. Yet, two methanogenic pathways are known to produce methane: CO_2 reduction and direct acetate dismutation (acetoclastic methanogenesis), which contribute to about 1/3 and 2/3 of biomethane production, respectively [17]. Here the possible involvement of exoelectrogenic bacteria and conductive materials in acetoclastic methanogenesis is unclear.

For instance, a review suggests that DIET-CO_2 reduction may not systematically explain the enhanced methane production by conductive materials [18]. Another insight suggesting the possible occurrence of other mechanisms is that DIET was evidenced only in cocultures of some electricigens, e.g. *Geobacter* spp., with methanogenic archaea, but major electroactive microorganisms such as *Geobacter* spp. are not always detected in improved methane production systems [19]. Two recent studies suggested that conductive magnetite accelerates acetoclastic methanogenesis [20,21]. First, Fu et al. showed that nanoFe_3O_4 acts as solid electron shuttles to accelerate acetoclastic methanogenesis by *Methanosarcina barkeri* in pure cultures [20]. Second, Inaba et al. provided metatranscriptomic evidence for stimulated acetoclastic methanogenesis by magnetite nanoparticle under continuous agitation [21]. These findings show that conductive minerals enhance the dismutation of acetate and, in turn, increase methanogenesis. Overall, these insights suggest that DIET-CO_2 reduction may not be the sole mechanisms explaining electromethanogenesis.

Until 2018, *Geobacter* spp. were the sole known bacterial species involved in DIET with methanogens [19]. Bioaugmentation of *Geobacter* has been shown to promote methanogenesis [22]. Yet *Geobacter* is in theory not the optimal species for syntrophy by acetoclastic methanogenesis because *Geobacter* can use acetate as a substrate, and, as a consequence, *Geobacter* and methanogens are in competition for acetate. Alternatively, other electroactive microorganisms such as *Shewanella* spp. may be involved [23,24]. For instance, *S. oneidensis* MR-1 consumes lactate to produce acetate and electrons [25], which are substrates for methanogens. Therefore, there may be a potential syntrophy between *Shewanella* and methanogens by acetoclastic methanogenesis. However, strong experimental evidence is actually missing, despite observations of the co-occurrence of both *Shewanella* and methanogens in some environments [26,27].

Here we investigated the role of *S. oneidensis* on acetoclastic methanogenesis. We mainly focused on three points: 1, potential syntrophy: whether bioaugmentation of *S. oneidensis* MR-1 can enhance methane production; 2, electric syntrophy: whether the increased methane production performance is related to exoelectrogenic activity; 3, we hypothesized that methane production by acetoclastic methanogenesis stimulated by *S. oneidensis* MR-1 and carbon materials acts as an alternative to classical CO_2 reduction. The following sections present results on methane production, exoelectrogenic activity, microbial diversity, thermodynamics, and ^{13}C tracing.

2. Materials and methods

2.1. Bacteria growth and inoculation

Experiment 1: Luria–Bertani (LB) broth was inoculated with *S. oneidensis* MR-1 and incubated aerobically at 30 °C until the optical density (OD600) reached 2. Then, *S. oneidensis* MR-1 was included into new broth with a nitrogen blowing in advance to adapt anaerobic growth. The bacterial culture of about 100 mL was concentrated by refrigerated centrifugation at 6000 rpm and 4 °C in an anaerobic glove box (Coy Laboratory Products). The collected cells were dissolved in 1 mL oxygen-free phosphate buffer saline solution (50 mM, pH 7.2) as a seed solution.

2.2. Soil sample and batch experiments (Experiment 2)

We sampled a soil from the Yellow River Delta [28,29]. *S*traw was thus used as the carbon source during pre-incubation for enriching methanogenic archaea. In brief, 150 g soil, 1.5 g straw and 450 mL sterile water were poured into a 1000 mL serum bottle. The bottles were flushed 30 min with high-purity N_2 then incubated statically at 30 °C in the dark for five weeks. For *S. oneidensis* MR-1, its nearly inability for anaerobic acetate metabolism provided advantage that this kind of electricigens does not compete with methanogens for acetate [23]. During pre-incubation, the potential electron acceptors, such as sulfate and nitrate, are consumed accompanied by high amounts of methane production, of about 100,000 ppm.

Bioaugmentation was performed by adding 0.1 mL of *S. oneidensis* MR-1 seed solution, obtained from experiment 1, into each vial with the total volume about 11 mL. The volume occupied by the slurry and upper space is approximately 5.5 mL, respectively. The other treatment groups were vials with granular activated carbon (GAC) or carbon nanotubes (CNTs). Characterization of GAC is given by Liu et al. [6]. The final amount of GAC was 1 g/L. CNTs were characterized by scanning electron microscope (SEM), indication a diameter in the nanometer range (Fig. S1). For the experiments including CNTs, suspensions of 10 g/L CNTs in ultrapure water were N_2 flushed, then sterilized. CNTs suspension (100 μL) was added to vials with a total volume of 11 mL to reach a concentration of about 0.2 g/L. Other treatments including the control group, *S. oneidensis* MR-1 and GAC treatment received equal amount of oxygen-free and sterilized ultrapure water (0.1 mL). Acetate was used as the substrate for methanogens with the final acetate concentration about 20 mM according to a previous report [30]. Overall, all treatments contained the same amount of upper space and slurry

plus with sterile water about 5.5 mL.

Vials were sacrificed in triplicate to measure the concentrations of methane, hydrogen and CO_2 after 1, 2, 3, 4, 5, 6, 7 and 8 days of incubation with a gas chromatography (GC; Agilent 7820A, USA) equipped with a flame ionization detector (FID) and a thermal conductivity detector (TCD). The column is Hayesep Q 80–100 mesh (6ft*1.8″* 2.0 mm). The low detection limits for methane and hydrogen are respectively 0.0008 mM and 0.0004 mM. High-pressure liquid chromatography (HPLC; Agilent 1260 Infinity) was used to measure the acetate concentration, with a minimum detectable limit of 0.02 mM.

2.3. Batch experiments for identifying methanogenic pathways by inhibitor

Experiment 3: CH_3F, an inhibitor of acetoclastic methanogenesis [17], was applied at 1.5%v/v in N_2 in the vials to distinguish the respective contribution of acetoclastic methanogenesis and CO_2 reduction to total methane production. In addition to replacing the same amount of nitrogen with 1.5% CH_3F gas, other operations can refer to experiment 2.

2.4. Carbon stable isotope fractionation for identifying methanogenic pathways

Experiment 4: Carbon stable isotope fractionation and the related calculations were conducted as well. CH_4 and CO_2 collected from the headspace were tested for obtaining the $\delta^{13}C$ using a gas chromatograph combustion isotope ratio mass spectrometer (GC–C–IRMS) system (Thermo Fisher MAT253, Germany). The isotopes were quantified with a Finnigan MAT253 IRMS. Separation of CH_4/CO_2 was performed in a Finnigan Precon. Gas (~1mL) was injected into a sample container (100 mL), which was filled with helium gas (99.999% purity) beforehand. A chemical trap was applied to scrub CO_2 from the sample. Methane was subsequently purified by cold trap with the help of Ni wires. Then, methane can be oxidized in a combustion reactor at 960 °C and converted to CO_2 and water. The combusted CO_2 was enriched by two liquid nitrogen cold traps and transferred into the IRMS for determination. The precision of repeated analyses was ± 0.2‰ when 1.3 nmol methane was injected. The abundance of ^{13}C in a sample is given relative to a standard using the δ notation:

$$\delta^{13}C = \left[\left(\frac{^{13}C}{^{12}C} \right)_{sample} \Big/ \left(\frac{^{13}C}{^{12}C} \right)_{PDB} - 1 \right] \times 1000$$

where PDB refers to the Pee Dee Belemnite carbonate that is used as standard which has a $^{13}C/^{12}C$ ratio of 0.0112372. A similar method was used to test $\delta^{13}C$-values of CO_2. The chemical trap was replaced by a water trap. The α value can be calculated using the equation: $\alpha = \frac{\delta^{13}CO_2 + 1000}{\delta^{13}CH_4 + 1000}$. For the calculation of f_{ma}, the equation was used as follow, $f_{ma} = \frac{\delta_{mc} - \delta^{13}CH_4}{\delta_{mc} - \delta_{ma}}$.

2.5. ^{13}C tracing with high abundance of $^{13}CH_3COOH$

Experiment 5: some ^{13}C tracing experiments were conducted as well. Two kinds acetate with higher^{13}C-labelled methyl, 1% and 3% $^{13}C/^{12}C$, were spiked into vials, respectively, to follow the fate of the ^{13}C-labelled methyl. In addition to replacing $^{12}CH_3COOH$ with $^{13}CH_3COOH$, other operations can refer to experiment 2

2.6. 16S rRNA gene sequencing for archaea

Experiment 6: Archaeal (Arch519F and Arch915R) primers were used to perform amplification of the 16S rRNA gene. Three repetitions were carried out. An Illumina Miseq platform (Tiny Gene Bio-Tech (Shanghai) Co., Ltd.) was used for sequencing after the construction of the amplicon library. The OTU taxonomies (from phylum to species) were determined based on the NCBI database. The detailed analysis can refer to previous report [26].

2.7. Electrochemical analysis

Experiment 7: A microbial fuel cell (MFC) was used to analyze the electron transfer efficiency to study whether *S. oneidensis* MR-1 and conductive materials can accelerate electron output and transfer. H-type double chamber MFCs were used and the chambers were separated by a cation exchange membrane (Ultrex CMI-7000). A 3.0 cm × 2.5 cm × 0.3 cm graphite plate was used as the electrode in each chamber and connected with titanium wire. A1 kΩ resistor was equipped in the external circuit. N_2 was flushed 20 min in the two chambers to remove air. 80 mL of slurry, which came from the same batch incubations as experiment 2, was added in the anode chamber and 80 mL oxygen-free $K_3[Fe(CN)_6]$ (0.05 M) was added to the cathode chamber. For the treatments with bioaugmentation, *S. oneidensis* MR-1 was added in the anode chamber. N_2 was flushed 20 min again in the two chambers to remove air and methane produced by pre-incubated soil. A data acquisition system (Model 2700, Keithley Instruments, USA) and ExcellLINX software were used to record the output voltage. The current density, C_{den} (A/m^2) was calculated using the following expression: $C_{den} = U/RS$, where U is the output voltage (V), R is the external resistance (Ω), and S is the surface area of the electrodes (m^2). For batch experiments without electrode, it is reasonable that these electrons may be utilized by methanogens. For electrochemical impedance spectroscopy (EIS) test can referring to Xu et al. [31], the working electrode was anode, the cathode and Ag/AgCl electrode acted as the counter electrode and reference electrode, respectively. The EIS was conducted over a frequency range from 100 kHz to 0.01 Hz with a perturbation signal of 5 mV. The initial potential of EIS was the open circuit potential of MFCs. CVs were measured using an electrochemical workstation (CHI660e, Chenhua, China). Three electrodes were used same as EIS experiments. The working electrode had a scan voltage between − 1.2 and 2.0 V (versus Ag/AgCl), and the scan rates were 20 –140 mV/s.

2.8. Thermodynamic analysis

Experiment 8: Concentrations of gases and acetate were used to calculate the ΔG of hydrogenotrophic methanogenesis and acetoclastic methanogenesis. ΔG of hydrogenotrophic methanogenesis can be calculated as:

$$\Delta G = \Delta G^0 + RT * \left\{ \ln \left[\frac{C_{CH_4}}{(C_{CO_2} * C_{H_2}{}^4)} \right] \right\}$$

where ΔG^0 is ΔG at 273.15 K and 101.325 kPa; R, the ideal gas constant, 8.3145 $J{\cdot}mol^{-1}{\cdot}K^{-1}$; T, the absolute thermodynamic temperature, 303.15 K; C_{CH_4}, C_{CO_2}, and $C_{H_2}$are concentrations of methane, CO_2, and H_2, respectively, $mol{\cdot}L^{-1}$. The calculation of ΔG^0 was detailed referring to a previous study [28].

For acetoclastic methanogenesis, $\Delta G = \Delta G^0 + RT * \left\{ \ln \left[\frac{C_{CH_4} * C_{CO_2}}{C_{acetate}} \right] \right\} + 2.303 * RT * N_{pH}$ holds, where the parameters are the same as above. $C_{acetate}$ is concentration of acetate, $mol{\cdot}L^{-1}$; N_{pH} is pH value.

2.9. Statistical analysis

Data are presented as mean ± standard deviation of triplicate cultures expect for carbon isotope fractionation and calculation, in which two repetitions was conducted. All statistical analyses were performed with Origin 8.5 (Origin Lab Corporation, USA) software. T-test was used to analyze the significance level, and a P value < 0.05 was considered statistically significant.

3. Results and discussion

3.1. Potential electric syntrophy between S. oneidensis MR-1 and methanogens

3.1.1. Increase of methane production performance with S. oneidensis MR-1 and conductive GAC/CNTs

We incubated soil suspensions with the *S. oneidensis* MR-1 and two conductive materials: GAC and CNTs (experiment 2), with CH_3F (experiment 3). Results without CH_3F show that addition of *S. oneidensis* MR-1 increased the rate of methane production, of 0.88 mM/day, versus that of the control, of 0.76 mM/day ($p < 0.01$) (Fig. 1a, experiment 2). Further addition of conductive materials increased the rate of methane production to 1.06 mM/day for GAC and to 1.02 mM/day for CNTs ($p < 0.01$. Results also show that the addition of CH_3F highly inhibited methane production.

Our results reveal first that *S. oneidensis* MR-1 improved methane production. Indeed, although exoelectrogenic bacteria have been shown to favor DIET-mediated methane production [7,8,10], only *Geobacter* bacterial species have been found so far to participate in DIET with methanogens [19]. *Shewanella* species and methanogens have been previously detected simultaneously in the same niche [26,27], but no evidence was given for increasing methane production by exoelectrogenic activity. Second, the high increase of methane production by addition of conductive materials is explained by easier electron transfer between the electron donor *S. oneidensis* MR-1 and methanogens, thus suggesting an electric syntrophy. This hypothesis is strengthened by reports suggesting that carbon materials can act as electrode modifiers promoting direct electron transfer from *S. oneidensis* [32,33].

Third, the high decrease of methane production by addition of CH_3F demonstrates that acetate dismutation played a major role in methane production (Fig. 1a), beside the classical CO_2 reduction pathway. For instance, *S. oneidensis* MR-1 increased methane production only by 5% after 6 days of incubation with CH_3F, whereas the increase reached 22.5% without CH_3F. Calculations shows that acetoclastic methanogenesis accounted for 70–80% of produced methane, and, conversely, CO_2 reduction accounted for only 20–30% of produced methane (Table 1). Our findings are supported by pure culture and metatranscriptomic data showing that Fe_3O_4 nanoparticles act as electron shuttles to stimulate acetoclastic methanogenesis [20,21]. However, for this study and the two studies mentioned above [20,21], the experiments were performed with acetate as the sole carbon source. The observations may be limited to the simplified experimental conditions, not to real environments containing different VFAs (e.g., propionate and butyrate) and other organic compounds whose metabolism can involve DIET (via GAC or CNTs). But based on the results of this study, it reveals that acetoclastic methanogenesis is a major mechanism of methane production by electric syntrophy, versus the classical CO_2 reduction pathway. These findings are further strengthened by the analysis of electrical properties and methanogenic pathways in the next section.

3.1.2. Consistency of increased methane production and exoelectrogenic activity

We studied the electrochemical properties of soil suspensions with *S. oneidensis* MR-1 and conductive materials without CH_3F, using a microbial fuel cell (MFC) (experiment 7). Results show that *S. oneidensis* MR-1 highly increased the current density after 3 days of incubation (Fig. 2a). This finding is consistent with previous reports that current density showed significant improvement by *S. oneidensis* [24,34]. Moreover *S. oneidensis* MR-1 increased the electrical quantity to 123.0 C, versus 79.5 C in the control (Fig. 2b), and reduced the resistance from 597.7 to 516.5 Ω/cm^2 (Fig. 2c). This phenomenon has been explained by better electron transfer mediated by *S. oneidensis* C-type cytochromes [35,36]. Results also show that conductive materials further increased the current density, the electric quantity, and reduced the resistance by 46% for GAC and by 129% for CNTs. These findings are in agreement with the known increase of energy generation by electrogenic microbes when resistance is reduced [37,38]. Capacitance-voltage (CV) curves further show that *S. oneidensis* MR-1 increased the peak current value, and that CNTs induced the largest peak current (Fig. 2d and S2). This finding is in agreement with previous studies showing that GAC and CNTs enlarge the peak current [33,39].

It has been concluded that all microorganism are capable of extracellular electron transfer with electrodes with the ability of DIET to date [19]. Therefore, if the electron acceptor is a microorganism instead of electrode, it is very reasonable to occur an electric syntrophy process between *S. oneidensis* MR-1 and methanogens. Overall, our results imply that *S. oneidensis* MR-1 improved the exoelectrogenic activity and that conductive carbon materials further enhanced electron transfer. Specially, the perfect consistency between the increase of methane production (previous section) and exoelectrogenic activity by *S. oneidensis* MR-1 and GAC/CNTs strengthened the possibility that there is an electric syntrophy between *S. oneidensis* MR-1 and methanogens.

3.2. Population and abundance of archaea responding to the addition of S. oneidensis MR-1 and conductive materials

Methanosarcinaceae, which is the most metabolically versatile of the methanogenic archaea, had the highest abundance of archaea after

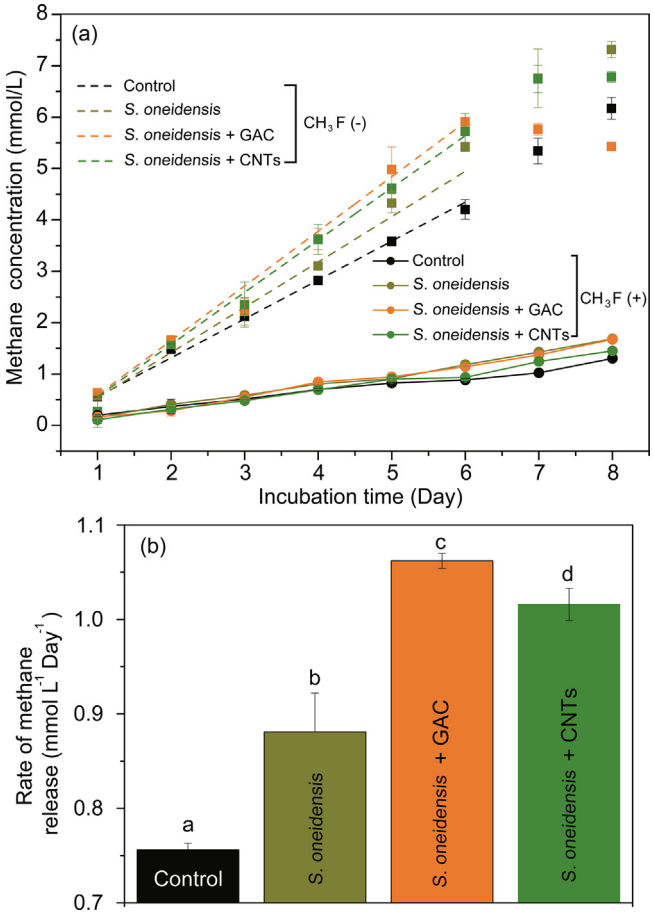

Fig. 1. Effects of *S. oneidensis* MR-1 and GAC/CNTs on methanogenic activities of wetland soils. (a) Time-courses of methane concentrations in the enrichment cultures in the absence or presence of CH_3F and (b) the methanogenic rates estimated from curves in (a). Where indicated, acetoclastic methanogenesis was inhibited by the addition of CH_3F. Different letters above the bar represent a significant difference ($p < 0.05$) in the methanogenic rates among different treatments. Data are presented as the means of three independent experiments, and error bars represent standard deviations.

Table 1
Isotopic signatures ($\delta^{13}C$) of CH_4 and CO_2 produced in the vials for the four treatments and fractions of acetate-dependent CH_4 production (f_{ma}) as calculated from $\delta^{13}C$-values of CH_4 and CO_2.

Sampling time	Treatments	$\delta^{13}C$-values of produced methane (with CH_3F)[1]	$\delta^{13}C$-values of produced CO_2 (with CH_3F)[2]	α[3]	$\delta^{13}C$-values of produced CO_2 (without CH_3F)[4]	$\delta^{13}CH_4$ (CO_2) i.e. δ_{mc}[5]	$\delta^{13}C$-values of produced CH_4 (without CH_3F) i.e. $\delta^{13}CH_4$	f_{ma} (%)[6]	(%)[7]
5th day	Control	−61.68 ± 2.13	−22.97 ± 0.81	1.044 ± 0.0	−20.65 ± 1.54	−64.15 ± 0.78	−51.27 ± 2.01	67.08	76.93
	S. oneidensis	−62.96 ± 3.65	−24.88 ± 0.84	1.045 ± 0.0	−20.47 ± 0.73	−66.87 ± 0.80	−50.94 ± 0.25	72.67	78.95
	S. oneidensis + GAC	−64.14 ± 0.90	−22.29 ± 1.26	1.046 ± 0.0	−21.28 ± 0.47	−65.29 ± 1.20	−50.94 ± 0.85	70.55	81.04
	S. oneidensis + CNTs	−63.79 ± 2.09	−23.12 ± 1.36	1.045 ± 0.0	−22.02 ± 0.15	−65.18 ± 1.31	−48.53 ± 2.84	82.30	80.43
6th day	Control	−60.83 ± 0.11	−23.28 ± 0.31	1.041 ± 0.0	−22.45 ± 0.38	−61.75 ± 0.30	−49.39 ± 0.54	73.57	78.96
	S. oneidensis	−65.17 ± 0.40	−22.75 ± 0.23	1.045 ± 0.0	−23.36 ± 0.29	−64.83 ± 0.22	−48.39 ± 0.33	82.70	78.16
	S. oneidensis + GAC	−64.84 ± 1.53	−22.86 ± 0.58	1.045 ± 0.0	−22.45 ± 0.76	−64.93 ± 0.55	−46.10 ± 1.03	94.24	80.67
	S. oneidensis + CNTs	−62.09 ± 0.56	−22.70 ± 0.41	1.043 ± 0.0	−21.97 ± 1.57	−62.99 ± 0.39	−46.06 ± 0.21	93.85	83.65

[1,2] $\delta^{13}C$-values of CH_4 and CO_2 produced in incubations of slurry in the presence of CH_3F.
[3] Calculated with the equation $\left(\alpha_{CO_2/CH_4}=\frac{\delta^{13}Co_2+1000}{\delta^{13}CH_4(Co_2)+1000}\right)$ using $\delta^{13}C$-values of CH_4 and CO_2 in the presence of CH_3F.
[4] $\delta^{13}C$-values of CO_2 produced in incubations of slurry without CH_3F.
[5] Calculated values of $\delta^{13}CH_4$ using ([3]) and ([4]) according to the equation shown in ([3]).
[6] According to a previous review [50], the value of δ_{ma} was calculated by assuming an ε of −21‰ and $\delta_{ma} = \delta^{13}$Cacetate + ε. Determined acetate value was −24.04 ± 0.23.
[7] The percentage of acetoclastic methanogenesis to the total methane from the direct measurement of methane production with or without the inhibitor (CH_3F).

the augmentation of *S. oneidensis* MR-1 (Fig. 3, experiment 6). Its abundance exceeded 62.2%. In sharp contrast, the abundance was only 8.63% in the control group. *S. oneidensis* MR-1 spurred a several-fold increase of Methanosarcinaceae abundance, reaching 7.21 times. Due to di-substrate consuming capacity of Methanosarcinaceae, we discussed in detail on the potential substrate, CO_2 or acetate, and syntrophic models in the next two parts.

The addition of GAC or CNTs resulted in a slight decrease in the abundance of Methanosarcinaceae, which is metabolically very versatile and capable of H_2/CO_2-utilizing methanogenesis. It is very interesting to note that both GAC and CNTs significantly improved the abundance of Methanosaetaceae, which is another methanogenic archaea via direct acetate dismutation to generate methane. The abundances in group of *S. oneidensis* MR-1, *S. oneidensis* MR-1 + GAC and *S. oneidensis* MR-1 + CNTs were 1.02, 14.33 and 5.15%, respectively. GAC and CNTs increased the multiple of Methanosaetaceae to 14.0 and 5.05 times. It was reasonable that Methanosarcinaceae and Methanosaetaceae played an important role in methane production in this study. Very recently, we incubated of soils from a Fe(III)-rich red clay horizon and found that the abundances of *S. oneidensis* and Methanosarcinaceae were improved simultaneously [26]. The findings of this study explains well the experimental phenomena found in *in situ*

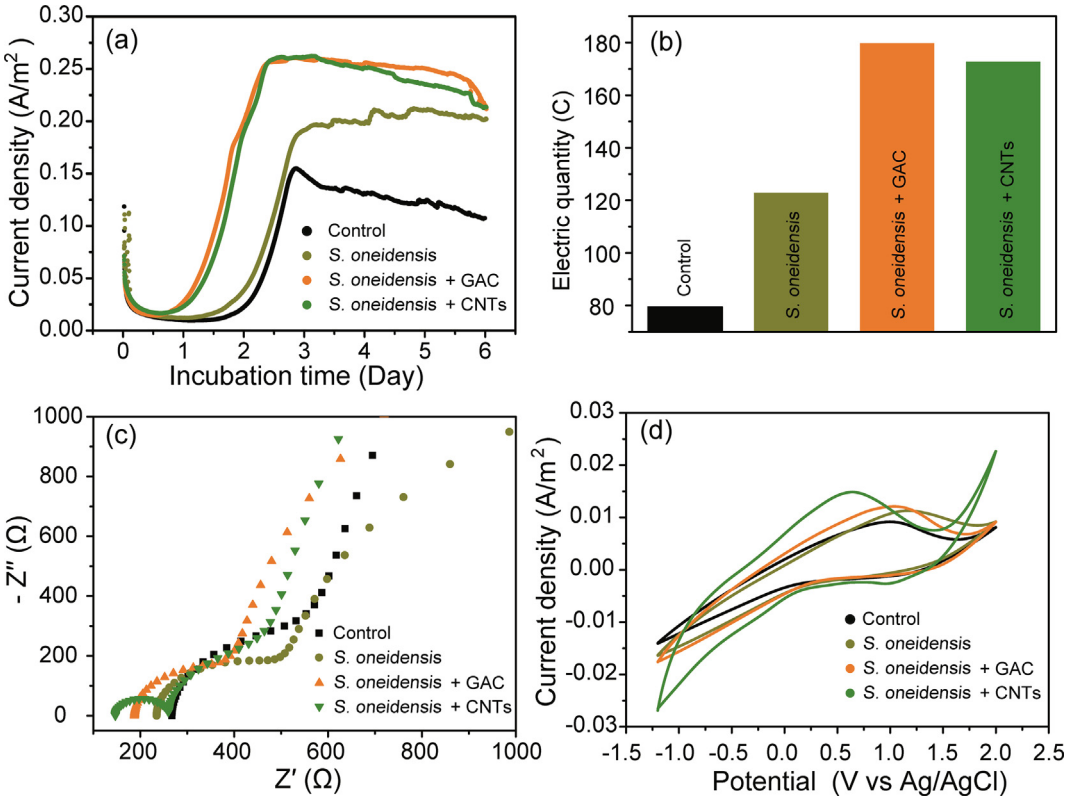

Fig. 2. Electrochemical characterizations of the performance of the MFC. Time-courses of current density (a) and the total electric quantity (b) in a 6-day experiment. The Nyquist plots (c) for the MFCs with the addition of *S. oneidensis* MR-1 and conductive GAC and CNTs. CVs at scan rate of 80 mV s^{-1} for four treatments (d).

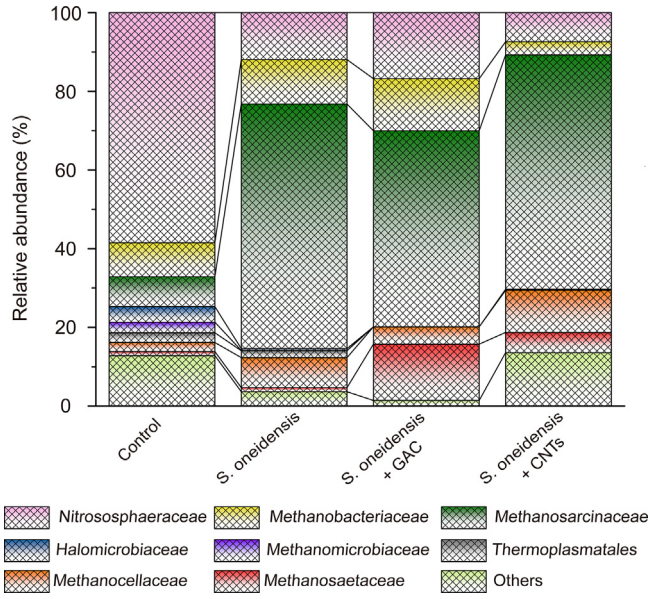

Fig. 3. Communities of archaea at the family level in incubated soil. Relative abundances of less than 1% for archaea were classified into the group 'others'.

environmental samples.

3.3. Identify major methanogenic pathways: Acetoclastic methanogenesis

3.3.1. Negligible contribution of CO_2 reduction for methane production by hydrogenotrophic methanogenesis

Hydrogen and electrons are the two most important reducing power to reduce CO_2. Hydrogen-producing microorganisms produced very little hydrogen (Fig. 4a, experiment 2). From the second day, hydrogen partial pressures were always below 1pa. The weak hydrogen-producing ability of related bacteria, such as negligible acetate oxidation progress, may cause this experimental phenomenon. It was found that threshold hydrogen partial pressure is generally greater than 10 Pa for hydrogenotrophic methanogenesis [2]. Even though the produced hydrogen can be completely converted to methane, the theoretical value is only about 0.113 μM methane. The detected methane concentration was four orders of magnitude of this theoretical value.

We further analyzed the potential contribution of hydrogenotrophic methanogenesis according to ΔG values (Fig. 4b, experiment 8 with data from experiment 2). The values of ΔG fluctuated around zero, and *S. oneidensis* MR-1 and conductive materials did change the trend of ΔG. This provides additional evidence that *S. oneidensis* MR-1 and carbon materials were not conducive to the hydrogenotrophic methanogenesis.

As reported, electrons can also directly reduce CO_2 to produce methane, which was more advantageous than hydrogen as electron carrier. It has been pointed out that external electron transfer rates per cell pair (cp) are considerably higher for DIET ($4.49*10^4$ e^- cp^{-1} s^{-1}) compared with hydrogen-mediated IET ($5.24*10^3$ e^- cp^{-1} s^{-1}) using a reaction–diffusion-electrochemical approach in a three-dimensional domain [40]. Therefore, we tried to analyse that whether the ignorable contribution of hydrogenotrophic methanogenesis was due to the more robust of direct electron transfer. Analysis of interspecies electron transfer via hydrogen diffusion can be reliable with reference to Cruz Viggi et al. [41]. The calculated value of i_{H_2} is about 1×10^{-11} A (data from experiment 2). As showed in Fig. 2a, the maximum current intensity detected by electrochemical workstation in the range 4.8×10^{-4} A, which was much higher than i_{H_2}. Direct utilization of H_2 as reducing power to generate methane seemed to be negligible in this study.

3.3.2. *S. oneidensis* MR-1 triggered slight CO_2 reduction with electrons as reducing power compared to direct acetate dismutation

Acetoclastic methanogenesis is much more sensitive to CH_3F compared to other methanogenic pathways. *S. oneidensis* MR-1 was not to be more beneficial to CO_2 reduction in this study. For the effects of *S. oneidensis* MR-1 on methanogenic pathway, the proportion of methane from CO_2 reduction was the highest with values about 23.07% (=100%-76.93%) and 21.04% (=100%-78.96%) in the control group (Table 1), and *S. oneidensis* MR-1 diminished the importance of CO_2 reduction to produce methane (Table 1). Therefore, the generated electrons may be more shunted to the acetate dismutation pathway with the presence of *S. oneidensis* MR-1.

GAC did not accelerate CO_2 reduction, and CNTs even showed a negative impact on CO_2 reduction. In contrast, an obvious promotion occurred when direct acetate dismutation pathway was involved (Fig. 1a). However, when the source of methane production is not analyzed in detail, overwhelming researches suggested that the enhancement of methane production is from an increase of CO_2 reduction [10,15,42,43]. According to the detailed analysis, this study showed that electromethanogenesis may come from the acetoclastic methanogenesis as an alternative to DIET-CO_2 reduction.

3.4. *S. oneidensis* MR-1 and GAC/CNTs stimulated acetoclastic methanogenesis

3.4.1. Thermodynamically favorable for acetoclastic methanogenesis

ΔG of acetoclastic methanogenesis was also analyzed (Fig. 5b,

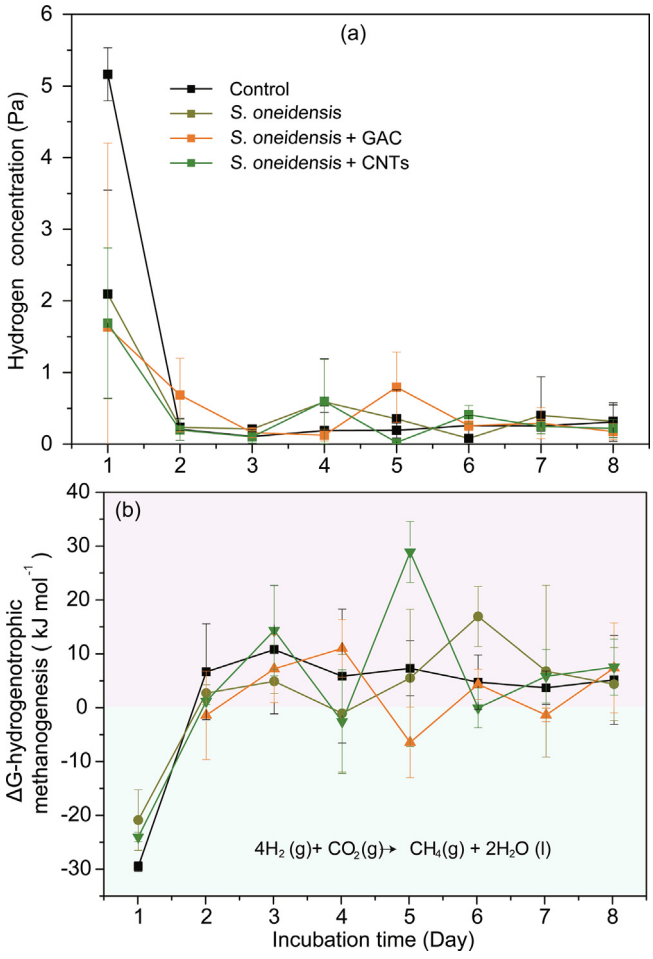

Fig. 4. Dynamics of hydrogen (a) and the ΔG values for hydrogenotrophic methanogenesis (b) within the batch experiment fed with acetate. Error bars represent standard deviations of triplicate tests.

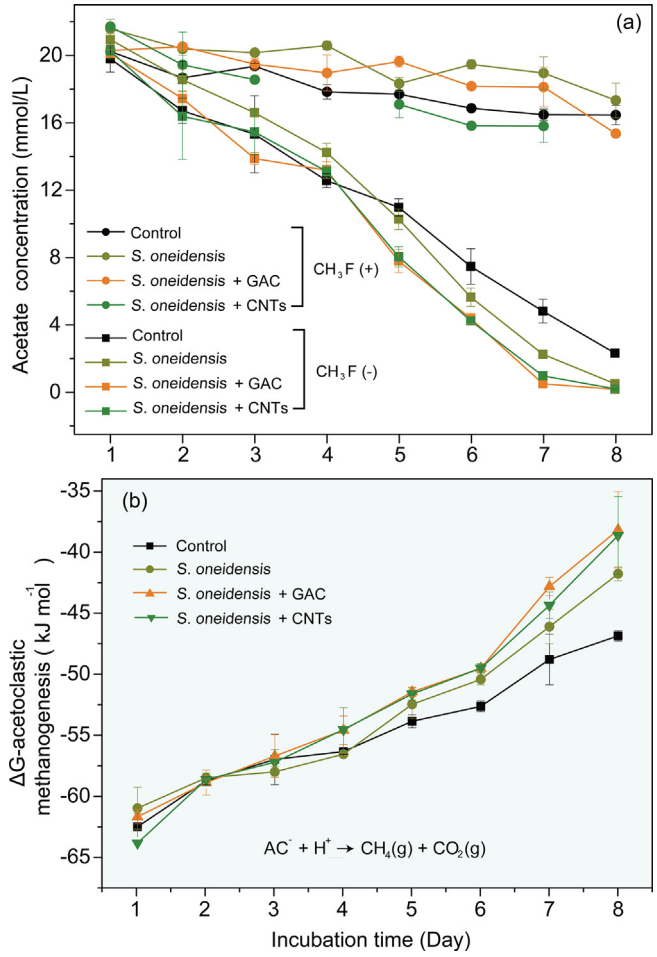

Fig. 5. Dynamics of acetate within the batch experiment (a) and the ΔG values for acetoclastic methanogenesis (b). Error bars represent standard deviations of triplicate tests.

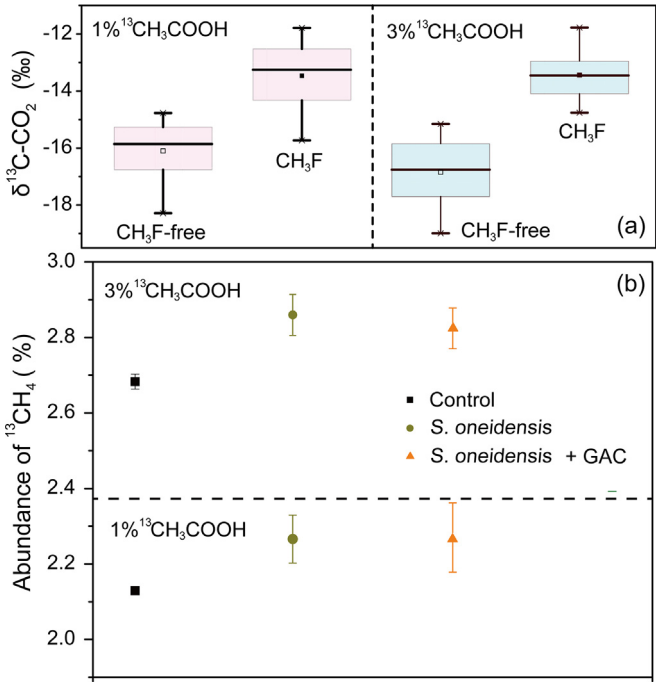

Fig. 6. Abundance of $^{13}CO_2$ and $^{13}CH_4$ with the application of 1% and 3% $^{13}CH_3COOH$. (a) $^{13}CO_2$ of the four treatments in the presence or absence of CH_3F; (b) abundance of $^{13}CH_4$ affected by *S. oneidensis* MR-1 and conductive GAC.

experiment 8 with data from experiment 2). Although ΔG gradually became larger due to the decrease of acetate concentration and increase of methane concentration, the values of ΔG during the whole process were still negative, which indicates that this pathway can occur spontaneously. Moreover, if the physiological activities of methanogens and energy release are comprehensively considered, direct acetate dismutation actually generates more energy than CO_2 reduction in a nominal environment detailed in a previous study [44]. In brief, for generating one mole of methane, 32 or 1 kJ of energy is available by acetoclastic methanogenesis or hydrogenotrophic methanogenesis, respectively, to *Methanosarcina*. This requirement may also be why the proportion of methane production from acetate dismutation, ~80%, was much higher than that from CO_2 reduction, ~20%, at the condition with sufficient acetate supply. In fact, with low concentration of acetate supply, an increase of electron transfer seemed to be still favorable to CO_2 reduction [45].

3.4.2. Consistency of direct acetate dismutation and methane production by carbon balance analysis

No significant difference existed for acetate consumption in the first half of the experiment (Fig. 5a, experiment 2). Correspondingly, *S. oneidensis* MR-1 and GAC/CNTs did not cause more methane production (Fig. 1a). In the second half, the rate of acetate decrease was enhanced by *S. oneidensis* MR-1. GAC and CNTs stimulated acetate utilization to a greater extent compared with only *S. oneidensis* MR-1 addition with significant statistical differences ($p < 0.01$ at 4th, 5th and 6th day) (Fig. 5a). It is worth emphasizing, trend of methane production was in compliance with acetate consumption. *S. oneidensis* MR-1 significantly promoted methane production ($p < 0.01$ at 4th, 5th and 6th day), and in particular, GAC and CNTs further accelerated methane accumulation. Moreover, the time node at which the current density reached the maximum was basically consistent with the max difference of acetate consumption and the methane production for all four treatments, suggesting that electricity may play a very important role in the direct utilization of acetate to perform methanogenesis.

3.4.3. Carbon stable isotope fractionation and calculation confirmed a significant contribution of acetoclastic methanogenesis

To further confirm that produced methane mainly derived from direct acetate dismutation, the ^{13}C of methane and CO_2 were analyzed on the 5th and 6th days (experiment 4, data from experiment 2 and 3), when the obvious difference of methane concentration presented. Inhibition of acetoclastic methanogenesis resulted in lower $\delta^{13}C$-CH_4 (Table 1). The $\delta^{13}C$-CH_4 in the presence of CH_3F represents the $\delta^{13}C$ of methane from CO_2 reduction ($\delta^{13}CH_4(CO_2)$, i.e. δ_{mc}) [17]. δ_{mc} is expected of being lower than the $\delta^{13}C$ of total methane, which was actually observed. The fractionation factors of CO_2 reduction, α, were in a range of 1.041–1.046, which have been observed in anaerobic soils [46,47]. Specially, Krüger et al. showed that adding straw obviously affected the α value [47], which was about 1.04 compared to 1.07 without straw. It was very similar to the results showed in table 1 ($\alpha = 1.041–1.046$). The same range of α value has been used for calculation of f_{ma} during study on rice fields and laboratory study [46,48].

On the fifth day, the proportion of produced methane from acetate dismutation was 67.08% in the control group (Table 1). *S. oneidensis* MR-1 and GAC and CNTs significantly increased the corresponding proportions to 72.67, 70.55 and 82.50%, respectively. Similarly, on the sixth day, the proportion in the control group was 73.57% by acetoclastic methanogenesis, and *S. oneidensis* MR-1 increased by nearly 10 percentage points to 82.70%. In particular, it increased again by more than 10% to 94.24 and 93.85% with the application of GAC and CNTs. Obviously, methane was mainly from direct acetate dismutation and further enhanced by *S. oneidensis* MR-1. More importantly, conductive

materials further facilitated the completion of this process. It was also observed that conductive materials increased the proportion of acetoclastic methanogenesis in anaerobic granular sludge [49]. Overall, the two methods, inhibitor and natural abundance stable isotope fractionation, reached perfectly consistent conclusions. For acetoclastic methanogenesis, methanogenic archaea convert acetate into methane and CO_2 by dismutation reaction ($CH_3COO^- + H^+ \rightarrow CH_4 + CO_2$). Here, the acetate carboxyl group is oxidized to CO_2 with the release of electrons ($COOH^- \rightarrow CO_2 + e^- + H^+$). Then, electrons are used to reduce methyl groups to form CH_4 ($CH_3^- + e^- + H^+ \rightarrow CH_4$). It is reported that magnetite nanoparticles penetrate into the cell membrane of *M. barkeri* to function as a solid electron shuttle [20]. GAC is a large particle carbon-based material that cannot penetrate into the cell membrane. Our previous research found that GAC can promote the syntrophic methane production between *Geobacter* and *Methanosarcina* by co-culture experiment [6]. In detail, GAC greatly stimulated ethanol metabolism and methane production in co-cultures of *Geobacter metallireducens* and *M. barkeri*. Cells were attached to GAC, but not closely aggregated, suggesting little opportunity for biological electrical contacts between the species when GAC acted as a "conductor". For the mechanisms/functions of GAC in this study, the biggest possibility is that GAC provided the attachment sites for *S. oneidensis* MR-1 and methanogens. The electrons released by *S. oneidensis* MR-1 are more easily transferred to the methanogens via GAC. As more exogenous electrons are provided, the reduction of methyl groups may be accelerated in this study, which further stimulates the rapid completion of the entire methanogenesis process.

3.4.4. Tracing of artificial carbon isotope verified the contribution of acetoclastic methanogenesis

The oxidation of carboxyl groups occurs firstly during the direct acetate dismutation, and the electrons produced in this process can reduce methyl groups to produce methane [1]. In theory, increasing the ratio of $^{13}CH_3COOH/^{12}CH_3COOH$ will enlarge the value of $^{13}CH_4$ produced by direct dismutation. Under the premise of inhibiting acetoclastic methanogenesis, the ^{13}C-CO_2 was improved for both treatments with artificial abundance of acetate (Fig. 6a, experiment 5), suggesting that part of the ^{13}C-labeled methyl group was oxidized to CO_2. This was consistent with the findings of natural abundance, which showed the occurrence of slight SAO (discussed in part 3.3.2). It should be noted that *S. oneidensis* MR-1 significantly enhanced the abundance of ^{13}C-CH_4 ($p < 0.05$) (Fig. 6b). It provided the robust evidence that exoelectrogenic bacteria can strengthen direct acetate dismutation. Carbon materials maintained a strong direct acetate dismutation capacity to make ^{13}C-CH_4 level stable. Collectively, direct acetate dismutation preference via increased electron donor and transfer presents an alternative strategy for syntrophic methanogenesis. For the potential for full-scale applications, this work implies that the process of direct acetate dismutation should be paid attention to when enhancing the methane production capacity of fermentation systems through bioaugmentation and/or conductive materials. For example, when a large amount of acetate accumulates due to the degradation of volatile fatty acids, in addition to strengthening syntrophic acetate oxidation coupled with CO_2 reduction to produce methane, the intervention of conductive materials to enhance the direct acetate dismutation pathway may also relieve the accumulation of acetate and even volatile fatty acids.

4. Conclusions

To date, long-standing concept that DIET-CO_2 reduction to generate methane introduced by conductive materials seems to be fully applicable to almost all scenario. Recently, some studies indicated the benefit of increased electron transfer on direct acetate dismutation [20,21,28]. However, these data are not enough to provide evidence that exoelectrogenic activity can affect direct acetate dismutation to generate methane. The findings in this study based on detailed experiments and confirmations expand electromethanogenic strategy that electric syntrophy, which can be strengthened by exoelectrogenic bacteria and electrical conductivity of carbon materials, can depend on acetoclastic methanogenic progress. Furthermore, for the first time, we tested the potential effect of *S. oneidensis* MR-1 on acetoclastic methanogenesis. This strategy can outcompete DIET-CO_2 reduction under some conditions with high acetate concentration. In addition to the well-known DIET-CO_2 reduction, this findings are very important complements to the strategy for biomethane production in natural environment and artificial anaerobic systems. Special for artificial fermentation with high-loading organic substance and acetate, more attention to the acetoclastic methanogenesis coupled with bioaugmentation by electroactive microorganisms is important for energy recovery.

Declaration of Competing Interest

The authors declare that they have no known competing financial interests or personal relationships that could have appeared to influence the work reported in this paper.

Acknowledgments

This research was financially supported by the National Natural Science Foundation of China (no. 41703075, 91751112 and 41573071), the Natural Science Foundation of Shandong Province, China (no. JQ201608 and ZR2016DQ12) and the Young Taishan Scholars Program (No. tsqn20161054).

Appendix A. Supplementary data

Supplementary data to this article can be found online at https://doi.org/10.1016/j.cej.2020.124469.

References

[1] P.N. Evans, J.A. Boyd, A.O. Leu, B.J. Woodcroft, D.H. Parks, P. Hugenholtz, G.W. Tyson, An evolving view of methane metabolism in the Archaea, Nat. Rev. Microbiol. 17 (2019) 219–232.
[2] R.K. Thauer, A.K. Kaster, H. Seedorf, W. Buckel, R. Hedderich, Methanogenic archaea: ecologically relevant differences in energy conservation, Nat. Rev. Microbiol. 6 (2008) 579–591.
[3] Y. Jeong, K. Cho, E.E. Kwon, Y.F. Tsang, J. Rinklebe, C. Park, Evaluating the feasibility of pyrophyllite-based ceramic membranes for treating domestic wastewater in anaerobic ceramic membrane bioreactors, Chem. Eng. J. 328 (2017) 567–573.
[4] A.J.M. Stams, C.M. Plugge, Electron transfer in syntrophic communities of anaerobic bacteria and archaea, Nat. Rev. Microbiol. 7 (2009) 568–577.
[5] M. Morita, N.S. Malvankar, A.E. Franks, Z.M. Summers, L. Giloteaux, A.E. Rotaru, C. Rotaru, D.R. Lovley, A. Casadevall, Potential for direct interspecies electron transfer in methanogenic wastewater digester aggregates, mBio 2 (4) (2011), https://doi.org/10.1128/mBio.00159-11.
[6] F. Liu, A.-E. Rotaru, P.M. Shrestha, N.S. Malvankar, K.P. Nevin, D.R. Lovley, Promoting direct interspecies electron transfer with activated carbon, Energy Environ. Sci. 5 (2012) 8982.
[7] A.E. Rotaru, P.M. Shrestha, F. Liu, M. Shrestha, D. Shrestha, M. Embree, K. Zengler, C. Wardman, K.P. Nevin, D.R. Lovley, A new model for electron flow during anaerobic digestion: direct interspecies electron transfer to Methanosaeta for the reduction of carbon dioxide to methane, Energy Environ. Sci. 7 (2014) 408–415.
[8] Q. Yin, X.Y. Zhu, G.Q. Zhan, T. Bo, Y.F. Yang, Y. Tao, X.H. He, D.P. Li, Z.Y. Yan, Enhanced methane production in an anaerobic digestion and microbial electrolysis cell coupled system with co-cultivation of *Geobacter* and *Methanosarcina*, J. Environ. Sci. China 42 (2016) 210–214.
[9] S.A. Cheng, D.F. Xing, D.F. Call, B.E. Logan, Direct biological conversion of electrical current into methane by electromethanogenesis, Environ. Sci. Technol. 43 (2009) 3953–3958.
[10] J.H. Park, H.J. Kang, K.H. Park, H.D. Park, Direct interspecies electron transfer via conductive materials: A perspective for anaerobic digestion applications, Bioresour. Technol. 254 (2018) 300–311.
[11] R. Mei, M.K. Nobu, T. Narihiro, J. Yu, A. Sathyagal, E. Willman, W.T. Liu, Novel *Geobacter* species and diverse methanogens contribute to enhanced methane production in media-added methanogenic reactors, Water Res. 147 (2018) 403–412.
[12] Y.Q. Lei, L.X. Wei, T.Y. Liu, Y.Y. Xiao, Y. Dang, D.Z. Sun, D.E. Holmes, Magnetite enhances anaerobic digestion and methanogenesis of fresh leachate from a municipal solid waste incineration plant, Chem. Eng. J. 348 (2018) 992–999.
[13] R.C. Lin, J. Cheng, L.K. Ding, J.D. Murphy, Improved efficiency of anaerobic

digestion through direct interspecies electron transfer at mesophilic and thermophilic temperature ranges, Chem. Eng. J. 350 (2018) 681–691.
[14] Z. Zhang, Y. Song, S. Zheng, G. Zhen, X. Lu, K. Takuro, K. Xu, P. Bakonyi, Electroconversion of carbon dioxide (CO_2) to low-carbon methane by bioelectromethanogenesis process in microbial electrolysis cells: The current status and future perspective, Bioresour. Technol. 279 (2019) 339–349.
[15] A.B.T. Nelabhotla, C. Dinamarca, Electrochemically mediated CO_2 reduction for bio-methane production: a review, Rev. Environ. Sci. Biotechnol. 17 (2018) 531–551.
[16] Z. Zhao, Y. Zhang, Y. Li, Y. Dang, T. Zhu, X. Quan, Potentially shifting from interspecies hydrogen transfer to direct interspecies electron transfer for syntrophic metabolism to resist acidic impact with conductive carbon cloth, Chem. Eng. J. 313 (2017) 10–18.
[17] R. Conrad, Quantification of methanogenic pathways using stable carbon isotopic signatures: a review and a proposal, Org. Geochem. 36 (2005) 739–752.
[18] G. Martins, A.F. Salvador, L. Pereira, M.M. Alves, Methane production and conductive materials: a critical review, Environ. Sci. Technol. 52 (2018) 10241–10253.
[19] C. Van Steendam, I. Smets, S. Skerlos, L. Raskin, Improving anaerobic digestion via direct interspecies electron transfer requires development of suitable characterization methods, Curr. Opin. Biotechnol. 57 (2019) 183–190.
[20] L. Fu, T. Zhou, J. Wang, L. You, Y. Lu, L. Yu, S. Zhou, NanoFe3O4 as solid electron shuttles to accelerate acetotrophic methanogenesis by Methanosarcina barkeri, Front. Microbiol. 10 (2019) 388.
[21] R. Inaba, M. Nagoya, A. Kouzuma, K. Watanabe, Metatranscriptomic evidence for magnetite nanoparticle-stimulated acetoclastic methanogenesis under continuous agitation, Appl. Environ. Microbiol. 85 (2019).
[22] S. Zhang, J.L. Chang, W. Liu, Y.R. Pan, K.P. Cui, X. Chen, P. Liang, X.Y. Zhang, Q. Wu, Y. Qiu, X. Huang, A novel bioaugmentation strategy to accelerate methanogenesis via adding *Geobacter sulfurreducens* PCA in anaerobic digestion system, Sci. Total Environ. 642 (2018) 322–326.
[23] B.E. Logan, R. Rossi, A. Ragab, P.E. Saikaly, Electroactive microorganisms in bioelectrochemical systems, Nat. Rev. Microbiol. 17 (2019) 307–319.
[24] B.R. Ringeisen, E. Henderson, P.K. Wu, J. Pietron, R. Ray, B. Little, J.C. Biffinger, J.M. Jones-Meehan, High power density from a miniature microbial fuel cell using *Shewanella oneidensis* DSP10, Environ. Sci. Technol. 40 (2006) 2629–2634.
[25] Y.J.J. Tang, A.L. Meadows, J.D. Keasling, A kinetic model describing Shewanella oneidensis MR-1 growth, substrate consumption, and product secretion, Biotechnol. Bioeng. 96 (2007) 125–133.
[26] L. Xiao, W. Wei, M. Luo, H. Xu, D. Feng, J. Yu, J. Huang, F. Liu, A potential contribution of a Fe(III)-rich red clay horizon to methane release: Biogenetic magnetite-mediated methanogenesis, Catena 181 (2019) 104081.
[27] N. Guo, X.F. Ma, S.J. Ren, S.G. Wang, Y.K. Wang, Mechanisms of metabolic performance enhancement during electrically assisted anaerobic treatment of chloramphenicol wastewater, Water Res. 156 (2019) 199–207.
[28] J. Li, L. Xiao, S. Zheng, Y. Zhang, M. Luo, C. Tong, H. Xu, Y. Tan, J. Liu, O. Wang, F. Liu, A new insight into the strategy for methane production affected by conductive carbon cloth in wetland soil: Beneficial to acetoclastic methanogenesis instead of CO_2 reduction, Sci. Total Environ. 643 (2018) 1024–1030.
[29] L. Xiao, B. Xie, J. Liu, H. Zhang, G. Han, O. Wang, F. Liu, Stimulation of long-term ammonium nitrogen deposition on methanogenesis by Methanocellaceae in a coastal wetland, Sci. Total Environ. 595 (2017) 337–343.
[30] D. Wagner, A. Lipski, A. Embacher, A. Gattinger, Methane fluxes in permafrost habitats of the Lena Delta: effects of microbial community structure and organic matter quality, Environ. Microbiol. 7 (2005) 1582–1592.
[31] H.D. Xu, X.C. Quan, Z.T. Xiao, L. Chen, Effect of anodes decoration with metal and metal oxides nanoparticles on pharmaceutically active compounds removal and power generation in microbial fuel cells, Chem. Eng. J. 335 (2018) 539–547.
[32] J. Liu, F. Zhang, W.H. He, X.Y. Zhang, Y.J. Feng, B.E. Logan, Intermittent contact of fluidized anode particles containing exoelectrogenic biofilms for continuous power generation in microbial fuel cells, J. Power Sources 261 (2014) 278–284.
[33] L. Peng, S.J. You, J.Y. Wang, Carbon nanotubes as electrode modifier promoting direct electron transfer from *Shewanella oneidensis*, Biosens. Bioelectron. 25 (2010) 1248–1251.
[34] T. Liu, Y.Y. Yu, X.P. Deng, C.K. Ng, B. Cao, J.Y. Wang, S.A. Rice, S. Kjelleberg, H. Song, Enhanced Shewanella biofilm promotes bioelectricity generation, Biotechnol. Bioeng. 112 (2015) 2051–2059.
[35] A.A. Carmona-Martinez, F. Harnisch, L.A. Fitzgerald, J.C. Biffinger, B.R. Ringeisen, U. Schroder, Cyclic voltammetric analysis of the electron transfer of *Shewanella oneidensis* MR-1 and nanofilament and cytochrome knock-out mutants, Bioelectrochem. 81 (2011) 74–80.
[36] V.R. Nimje, C.Y. Chen, H.R. Chen, C.C. Chen, Y.M. Huang, M.J. Tseng, K.C. Cheng, Y.F. Chang, Comparative bioelectricity production from various wastewaters in microbial fuel cells using mixed cultures and a pure strain of *Shewanella oneidensis*, Bioresour. Technol. 104 (2012) 315–323.
[37] B.E. Logan, Exoelectrogenic bacteria that power microbial fuel cells, Nat. Rev. Microbiol. 7 (2009) 375–381.
[38] C. Zhao, C. Yu, B. Qiu, S. Zhou, M. Zhang, H. Huang, B. Wang, J. Zhao, X. Sun, J. Qiu, Ultrahigh Rate and Long-Life Sodium-Ion Batteries Enabled by Engineered Surface and Near-Surface Reactions, Adv. Mater. 30 (2018) 1702486.
[39] X.M. Zhang, M. Epifanio, E. Marsili, Electrochemical characteristics of *Shewanella loihica* on carbon nanotubes-modified graphite surfaces, Electrochim. Acta 102 (2013) 252–258.
[40] T. Storck, B. Virdis, D.J. Batstone, Modelling extracellular limitations for mediated versus direct interspecies electron transfer, ISME J. 10 (2016) 621–631.
[41] C.C. Viggi, S. Rossetti, S. Fazi, P. Paiano, M. Majone, F. Aulenta, Magnetite particles triggering a faster and more robust syntrophic pathway of methanogenic propionate degradation, Environ. Sci. Technol. 48 (2014) 7536–7543.
[42] Q. Yin, S. Yang, Z. Wang, L. Xing, G. Wu, Clarifying electron transfer and metagenomic analysis of microbial community in the methane production process with the addition of ferroferric oxide, Chem. Eng. J. 333 (2018) 216–225.
[43] X. Song, J. Liu, Q. Jiang, P. Zhang, Y. Shao, W. He, Y. Feng, Enhanced electron transfer and methane production from low-strength wastewater using a new granular activated carbon modified with nano-Fe_3O_4, Chem. Eng. J. 374 (2019) 1344–1352.
[44] C.M. Bethke, R.A. Sanford, M.F. Kirk, Q.S. Jin, T.M. Flynn, The Thermodynamic Ladder in Geomicrobiology, Am. J. Sci. 311 (2011) 183–210.
[45] L. Xiao, F. Liu, J. Liu, J. Li, Y. Zhang, J. Yu, O. Wang, Nano-Fe_3O_4 particles accelerating electromethanogenesis on an hour-long timescale in wetland soil, Environ, Sci. Nano 5 (2018) 436–445.
[46] H. Penning, R. Conrad, Quantification of carbon flow from stable isotope fractionation in rice field soils with different organic matter content, Org Geochem. 38 (2007) 2058–2069.
[47] M. Kruger, Seasonal variation in pathways of CH_4 production and in CH_4 oxidation in rice fields determined by stable carbon isotopes and specific inhibitors, Glob. Change Biol. 2002 (2002) 265–280.
[48] R. Susilawati, S.D. Golding, K.A. Baublys, J.S. Esterle, S.K. Hamilton, Carbon and hydrogen isotope fractionation during methanogenesis: A laboratory study using coal and formation water, Int. J. Coal Geol. 162 (2016) 108–122.
[49] L. Xiao, R. Sun, P. Zhang, S. Zheng, Y. Tan, J. Li, Y. Zhang, F. Liu, Simultaneous intensification of direct acetate cleavage and CO_2 reduction to generate methane by bioaugmentation and increased electron transfer, Chem. Eng. J. 378 (2019) 122229.
[50] M. Whiticar, Carbon and hydrogen isotope systematics of bacterial formation and oxidation of methane, Chem. Geol. 161 (1999) 291–314.

Supplementary Material

Methane production by acetate dismutation stimulated by *Shewanella oneidensis* and carbon materials: As an alternative to classical CO_2 reduction

Leilei Xiao[1,3], Fanghua Liu[1,2,3]*, Eric Lichtfouse[4], Peng Zhang[5], Dawei Feng[1,3], Fangbai Li[6]

Chemical Engineering Journal, Volume 389, 1 June 2020, 124469

https://doi.org/10.1016/j.cej.2020.124469

[1] Key Laboratory of Coastal Biology and Biological Resources Utilization, Yantai Institute of Coastal Zone Research, Chinese Academy of Sciences, Yantai 264003, P.R. China;
[2] Laboratory for Marine Biology and Biotechnology, Qingdao National Laboratory for Marine Science and Technology, Qingdao, 266237, P.R. China;
[3] Center for Ocean Mega-Science, Chinese Academy of Sciences, Qingdao 266071, P.R. China;
[4] Aix-Marseille Univ, CNRS, IRD, INRA, Coll France, CEREGE, Avenue Louis Philibert, Aix en Provence 13100, France;
[5] Faculty of Environmental Science & Engineering, Kunming University of Science & Technology, Kunming 650500, P.R. China;
[6] Guangdong Key Laboratory of Integrated Agro-environmental Pollution Control and Management, Guangdong Institute of Eco-environmental Science & Technology, Guangzhou, 510650, China.

* To whom correspondence should be sent:
Fanghua Liu, Yantai Institute of Coastal Zone Research, 17 Chunhui Road, Laishan District, Yantai, Shandong 264003, China. Office number: +86 05352109268, Email: fhliu@yic.ac.cn.

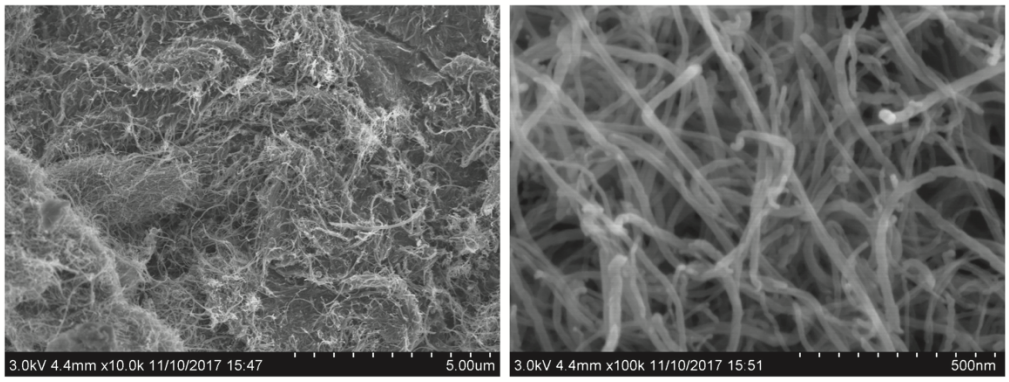

Figure S1. Carbon nanotube characterized by scanning electron microscopy.

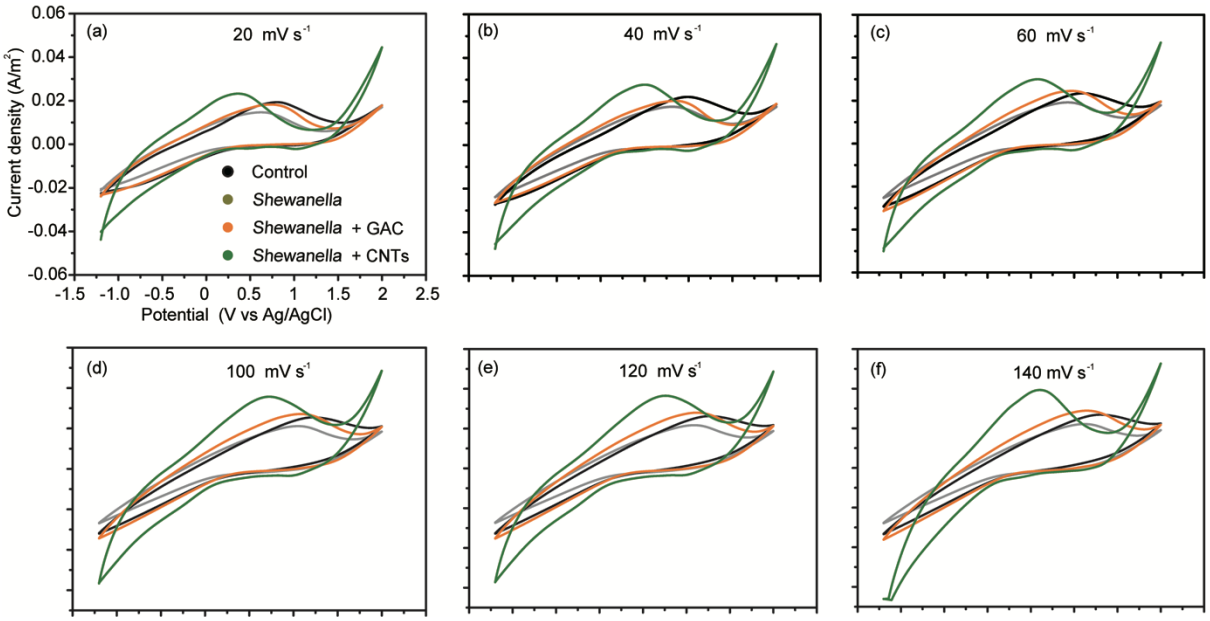

Figure S2. Capacitance voltage (CV) curves at various scan rates for four treatments. GAC: granular activated carbon, CNT: carbon nanotubes